Chemical Ionization Mass Spectrometry: Applications for the *In Situ* Measurement of Nonvolatile Organics at Ocean Worlds

Sarah E. Waller,* Anton Belousov,* Richard D. Kidd, Dragan Nikolić,
Stojan M. Madzunkov, Joshua S. Wiley, and Murray R. Darrach

Abstract

A new technique that has applications for the detection of nonvolatile organics on Ocean Worlds has been developed. Here, liquid mixtures of fatty acids (FAs) and/or amino acids (AAs) are introduced directly into a miniature quadrupole ion trap mass spectrometer (QITMS) developed at Jet Propulsion Laboratory and analyzed. Two ionization methods, electron impact and chemical ionization (EI and CI, respectively), are compared and contrasted. Further, multiple CI reagents are tested to explore their potential to ''soften'' ionization of FAs and AAs. Both EI and CI yield mass spectra that bear signatures of FAs or AAs; however, soft CI yields significantly cleaner mass spectra that are easier to interpret. The combination of soft CI with tandem mass spectrometry (MS/MS) has also been demonstrated for AAs, generating ''fingerprint'' mass spectra of fragments from protonated parent ions. To mimic potential Ocean World conditions, water is used as the primary collision gas in MS/MS experiments. This technique has the potential for the *in situ* analysis of molecules in the cryogenic plumes of Ocean Worlds (*e.g.*, Enceladus) and comets with the ultimate goal of detecting potential biosignatures. Key Words: Amino acids—Fatty acids—Chemical ionization—Mass spectrometry—Life detection—Ocean worlds. Astrobiology 19, xxx–xxx.

1. Introduction

Icy worlds have become a topic of great interest due to their potential for containing signs of extraterrestrial life. Since life as we know it requires liquid water, Ocean Worlds, such as Europa, Titan, Enceladus, Ganymede, and Callisto, have become astrobiological targets (Lunine, 2017). Four key requirements for habitability are liquid water, energy, carbon, and nitrogen (McKay *et al.*, 2014). Several of these Ocean Worlds present inhibitive challenges to habitability and the search for life. For example, Ganymede (Kivelson *et al.*, 2002) and Callisto (Anderson *et al.*, 1998) have deep underwater oceans that are isolated from their rocky cores by a layer of high-pressure ice, reducing the likelihood of hydrothermal chemistry. Further, the subsurface oceans are buried under several tens of kilometers of water ice and are not easily accessible.

Titan, on the other hand, has surface lakes and seas of liquid hydrocarbons, under which lies a liquid water ocean that is sandwiched between two layers of ice (Fortes, 2012). The top ice shell makes it difficult to access the liquid ocean, and the bottom ice shell isolates the liquid water from Titans's core.

Both Europa and Enceladus have subsurface oceans under an icy shell that come into contact with the moons' cores. The subsurface ocean of Enceladus may be accessed through a plume emanating from fractures at its southern pole (Porco *et al.*, 2006; Spahn *et al.*, 2006), and evidence is mounting for plume activity on Europa as well (Roth *et al.*, 2014; Sparks *et al.*, 2016; Jia *et al.*, 2018). Further, evidence of hydrothermal activity has been supported by the discovery of silica particles (Hsu *et al.*, 2015; Sekine *et al.*, 2015) and molecular hydrogen in Enceladus' plumes (Waite *et al.*, 2017). Choblet *et al.* (2017) have determined that tidal friction produces sufficient heat to support hydrothermal activity, with focused heating driving intense interactions between the liquid ocean and the rocky core and transporting hydrothermal products to the plume sources. As such, Enceladus and Europa represent some of the most reasonable targets in the search for extraterrestrial life.

The search for extinct or extant life on an Ocean World involves searching for specific molecules and molecular signatures that are representative of and unique to life. These molecules are termed biosignatures, and examples include

isotope patterns, the presence and ratios of chiral molecules, and the presence and distribution of organic molecules (Domagal-Goldman *et al.*, 2016; Hand *et al.*, 2017). For example, organic compounds from abiotic sources are typically composed of racemic mixtures of chiral molecules, branched chain isomers, show an exponential decline in the amount of molecules with increasing carbon number, and contain thermally stable and polycyclic aromatic hydrocarbons (Sephton and Botta, 2005).

On the other hand, organic compounds produced from organisms generally show a preference for chiral molecules in nonequilibrium ratios, straight chains or cyclic isomers, abundance patterns that differ from abiotic synthesis patterns, and the absence of thermally stable and polycyclic aromatic hydrocarbons (Sephton and Botta, 2005; Creamer *et al.*, 2017). The presence and characteristics of biomolecules such as amino acids (AAs) and fatty acids (FAs) are of particular interest (Johnson *et al.*, 2018). Specifically, the presence of AAs with a chiral imbalance and/or FA distribution patterns is not expected from abiotic synthetic pathways (Domagal-Goldman *et al.*, 2016).

There are two ways to search for biosignatures on Ocean Worlds. One is remotely, usually by spectroscopy conducted with telescopes orbiting the Earth (Norwood *et al.*, 2016). The other is by sending *in situ* instruments to locations of interest (Waite *et al.*, 2004; Rayman *et al.*, 2006; Leshin *et al.*, 2013; Postberg *et al.*, 2018; Webster *et al.*, 2018). Although there are many benefits to remote measurements, the main drawbacks of remote sensing from the Earth are that the techniques mostly probe species in the upper atmosphere, which are likely to be different to compounds on or near the surface, and that molecular species are not always able to be definitively identified due to spectral congestion (Encrenaz, 2008; Norwood *et al.*, 2016). Further, remote measurements tend to have lower sensitivity, making the detection of trace organic species nearly impossible. *In situ* instruments provide a direct analysis of the molecules present in and around potential habitable environments on an Ocean World.

Planetary missions can be divided into three categories: lander, orbiter, and flyby. There have been numerous orbital and flyby missions sent to planets (*e.g.*, Mars, Saturn, and Jupiter), moons (*e.g.*, Europa, Titan, and Enceladus), and comets (*e.g.*, Rosetta and Tempel 1) (Ball *et al.*, 2007; Gao and Chien, 2017). There have also been several lander missions; the most notable are the long lineage of landers and rovers sent to Mars (Ball *et al.*, 2007; Grotzinger *et al.*, 2012), the Huygens lander (Fulchignoni *et al.*, 2005; Tomasko *et al.*, 2005), and the Rosetta probe (Seidensticker *et al.*, 2007; Capaccioni *et al.*, 2015).

Depending on the type of body visited, landers typically drill or scrape the surface to collect a sample for analysis. Landers that drill or scrape the surface have been sent to comets (Rosetta) and planets (Mars) and have been proposed for missions to planets (Ceres) (Poncy *et al.*, 2008) and icy moons (Enceladus, Europa, and Titan) (Hand *et al.*, 2017). Landers can house more sophisticated instrumentation, such as separatory or chromatography-based techniques; however, sample collection can be more difficult and fraught with technical challenges (Hand, 2008; Arvidson *et al.*, 2009). Orbiters and flybys can pass through the coma or tail of a comet or the plumes of a moon (*e.g.*, Enceladus and possibly Europa) (Lorenz, 2016; Waite *et al.*, 2017) for sample collection and analysis with relative ease.

The Cassini-Huygens (Cassini) flybys of Enceladus have sparked intense interest in the search for biosignatures there due to its global subsurface salty ocean, the composition of which can be sampled in the cryovolcanic ice plumes that are ejected from the hidden subsurface ocean. Cassini made several passes through the ice plumes of Enceladus and by utilizing mass spectrometry (MS) found both simple (Waite *et al.*, 2006, 2009) and complex (Postberg *et al.*, 2018) organic compounds, some of which are biologically relevant. Further, H_2, CO_2, and CH_4 have been measured in Enceladus' plumes (Bouquet *et al.*, 2015; Waite *et al.*, 2017). It has also been suggested that Enceladus is home to all of the right ''ingredients'' to support life (Porco *et al.*, 2017).

One commonly used technique for extraterrestrial *in situ* instrumentation is MS, an analytical technique in which chemical species in a sample are ionized and separated based on their mass-to-charge (*m/z*) ratio. MS is a particularly powerful tool because it can yield specific mass information about the molecular species in a sample. This can be advantageous over rovibrational spectroscopic techniques, such as IR spectroscopy, which help identify functional groups in a sample but do not necessarily yield enough information for molecular identification.

Mass spectrometers have been most notably present on the Curiosity rover (Webster *et al.*, 2018), the Cassini spacecraft (Srama *et al.*, 2004; Waite *et al.*, 2004), the Huygens probe (Niemann *et al.*, 2005; Waite *et al.*, 2017), and the Rosetta orbiter (Balsiger *et al.*, 2007). Further, Europa Clipper, a future mission to visit the Jovian moons, will include two mass spectrometers: one to analyze contents of dust/ice contained in the exosphere or plumes, if they exist (Kempf *et al.*, 2014), and another to sample material ejected from potential plumes and the surface-sputtered atmosphere (Brockwell *et al.*, 2016; Sephton *et al.*, 2018).

One potential limitation to MS is the type of ionization used, which is often categorized as ''hard'' or ''soft.'' Hard ionization techniques, such as electron impact ionization (EI), impart excessive energy to sample molecules, often resulting in sample fragmentation. Electrospray ionization and chemical ionization (CI) are considered soft techniques and can cause little to no sample fragmentation. When a sample contains a complex mixture, soft ionization techniques are generally favored because they cause less fragmentation and thus yield mass spectra that are easier to interpret, allowing for more definitive molecular identification of sample constituents (Gross, 2011).

Tandem mass spectrometry (MS/MS) methods provide structural information and increased specificity and sensitivity beyond that contained in a full mass spectrum obtained with soft ionization only. Although EI is known for its ability to provide structural information when working with a pure sample, distinguishing fragment from parent ions as well as elucidating the parent ion of fragments is not practical in complex mixtures. For this reason, the combination of soft ionization followed by MS/MS is sometimes the only viable option for many real-world analyses if some form of chromatography or other separation technique does not precede MS, as may be the case for certain orbital and flyby missions.

The recent interest in Ocean Worlds and their potential habitability has made it necessary to develop *in situ* analytical techniques that are appropriate for water-based samples (Neish *et al.*, 2018). The detection and identification of potential biosignatures such as FAs and AAs is of

high priority, especially on Ocean Worlds (Johnson *et al.*, 2018). Due to their low vapor pressures, it is challenging to get FAs and AAs in the gas phase for ionization and detection. On an Ocean World such as Enceladus, volatile AAs may already exist in the gas phase in the plume; however, long-chain FAs and less volatile AAs entrenched within ice grains in the plume may volatilize after a high velocity impact between the ice grain and a surface. If the ice grain impacts an instrument surface, the species present in the grain can be characterized (Postberg *et al.*, 2009, 2011, 2018).

In this article, a technique for volatilizing, ionizing, and mass analyzing FAs and AAs directly in a miniature quadrupole ion trap mass spectrometer (QITMS) developed at the Jet Propulsion Laboratory (JPL) (Darrach *et al.*, 2010; Madzunkov and Nikolić, 2014; Madzunkov *et al.*, 2018) is presented, with hopes of eventually being implemented for the analysis of organics within ice grains during flybys of moon-like Enceladus.

A method for soft CI MS in water-rich environments has been developed and contrasted with EI MS. Due to the unavoidable presence of water (as a solid and/or gas) on Ocean Worlds, water was used as a reagent ion for CI as both a pure reagent and in mixtures with secondary reagent gases. Acetonitrile and acetone were also used as CI reagents to probe "softer" ionization conditions. Further, the ability to use water as a collision gas for MS/MS was explored. By taking advantage of the ability of the QITMS to perform single-stage and MS/MS, a method for FA and/or AA identification in aqueous samples has been demonstrated. Finally, the implementation of this technique (*i.e.*, CI followed by MS/MS) for a flight instrument is briefly discussed.

2. Materials and Methods

A schematic of a miniature QITMS developed at JPL (Madzunkov and Nikolić, 2014) is presented in Fig. 1. The QITMS comprised a Paul trap (Paul, 1990), a home-built electron impact ionization (EI) gun (filament: Kimball Physics,
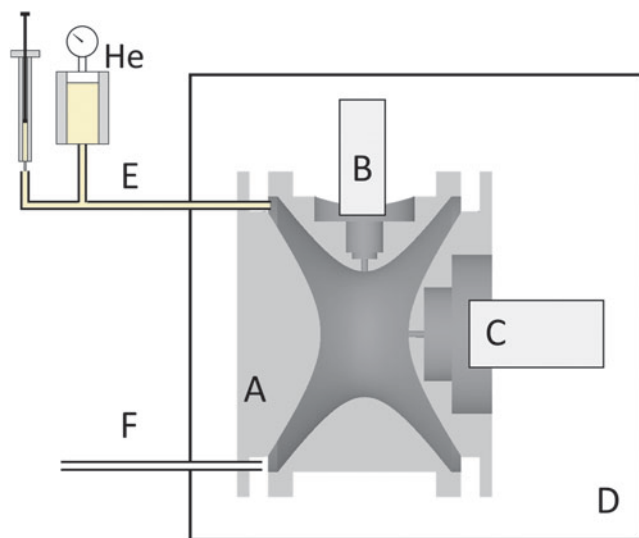

FIG. 1. Schematic of the experimental setup. A quadrupole ion trap mass spectrometer comprising a Paul trap (A), an electron gun ionizer (B), and a detector (C) is housed in a vacuum chamber (D). Liquid sample is introduced by a capillary connected to a syringe or a pressurizable reservoir (E). Gas can also be introduced into the trap by a tube (F).

ES-042), and a channel electron multiplier detector (Photonis, Magnum® 5901). The QITMS laboratory testbed instrument used in this study is housed in a 6 in. ConFlat® tee vacuum chamber. For this study, the electron ionization gun (Fig. 1B) is mounted to the ring electrode of the trap, as was done in a previous study (Avice *et al.*, 2019). Further, a capillary used to deliver a liquid sample is fed through a preexisting gas line and is positioned such that the end is ∼0.5 mm from the ring electrode. Similar techniques were considered as part of the vehicle cabin atmosphere monitor initiative and another JPL internally funded project; however, neither project selected a liquid injection technique.

The basics of quadrupole MS (March, 1997) and QITMS operation have been previously described in detail (Madzunkov and Nikolić, 2014). Briefly, the QIT comprised an inner ring electrode and two end-cap electrodes (Fig. 1A). The inner surfaces of the ring and end-cap electrodes are hyperbolic, and by applying a radio frequency (RF) electric potential to the ring electrode and grounding the two end-caps, a quadrupole electric field is created in the center of the ion trap. Ions above a particular *m/z* ratio are trapped in the quadrupole electric field, which is a function of, among other variables, the amplitude of the RF potential. The electronics that power the QITMS have been previously developed with commercial off-the-shelf electronic components chosen to have a viable path to flight (Schaefer *et al.*, 2008; Darrach *et al.*, 2015). A picture of the electronics module can be found in Supplementary Fig. S1.

The QITMS has a mass resolution (m/Δm) of 750 at 320 amu and a sensitivity of 10^{13} counts/torr/s (Avice *et al.*, 2019). To record a mass spectrum, the RF voltage magnitude is increased linearly, thus causing ions to be ejected from the trap from low to high *m/z*. Ions are ejected out of both end-caps; however, only ions ejected toward the end-cap with a channel electron multiplier are detected (Fig. 1C). In this way, a "full" mass spectrum is obtained.

MS/MS mass spectra can also be collected with this instrument. In MS/MS experiments, only ions of a particular *m/z* are trapped by ramping the RF amplitude to eject low *m/z* ions while simultaneously applying an AC voltage to the end-caps that resonantly ejects ions of higher *m/z* than the *m/z* of interest. Kinetic energy is then imparted to the trapped ions by adjusting the RF amplitude to create an appropriate potential well while introducing a supplemental AC voltage on the end-caps that is resonant with the secular frequency of the isolated ion. Collisions of the excited ions with neutral background gases added to the trap convert the kinetic energy into internal energy and result in fragmentation. For these experiments, water vapor is the supplied collision gas. The residual parent ions and resulting fragments are then ejected and detected, yielding an MS/MS mass spectrum.

In these experiments, a liquid solution is continuously deposited onto the ring electrode of the QIT through a silica capillary with an inner diameter (ID) of 10 or 15 μm and an outer diameter (OD) of 360 μm (Fig. 1E). The sample is pushed through the capillary from a syringe mounted in a syringe pump or from a liquid reservoir that can be pressurized up to 100 psia with helium gas (UHP; Airgas). The flow rate (50–200 nL/min) from the syringe pump or the He pressure with which the sample is introduced is used to control the pressure inside the trap. In addition, the ID of the fused silica capillary used for sample delivery can be varied to control the trap pressure. Gases may also be introduced

directly into the trap by a 0.040 in. ID, 1/16 in. OD (1.0 mm and 1.6 mm, respectively) stainless steel tube (Fig. 1F).
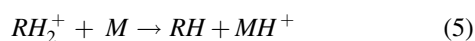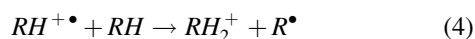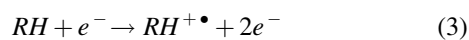
A thin layer of silicon (SilcoNert®; SilcoTek) coats the trap and gas line to reduce the adsorption of polar molecules onto the inner surfaces of the trap and tubing. The trap is heated by a halogen lamp to facilitate evaporation of the sample deposited in the QITMS. Typical operating temperatures of the trap are 115–125°C. Note that the sample introduction method described here would not be employed on a flight instrument. The focus of this article is to develop a CI method for future flight instrumentation. Rather, these methods are used for the ease with which they can be applied to a laboratory system. Ideally for a flight instrument, ice grains will be impact vaporized on the wall of the QITMS and molecular constituents mass analyzed. Heating the QITMS is useful, even in a flight-like scenario, as it helps prevent the loss of species through physisorption.

The target molecules introduced into the trap are primarily ionized in one of two ways. At low pressures ($<1 \times 10^{-6}$ torr), EI, where an electron with an energy of ~ 70 eV impinges on a neutral molecule causing electron loss and yielding a radical cation and two electrons, dominates (Bleakney, 1930). Note that 1 torr is equivalent to 1.3 mbar. EI is a high-energy process and after the initial ionization, the excited radical cation can then undergo secondary dissociation, resulting in fragmentation of the molecule. A simple nondissociative EI scheme followed by a dissociative scheme is shown next.

$$M + e^- \rightarrow M^{+\bullet *} + 2e^- \qquad (1)$$

$$M^{+\bullet *} \rightarrow D^+ + F^\bullet \qquad (2)$$
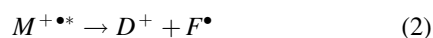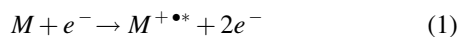
where M is the target molecule, $M^{+\bullet *}$ is a radical cation in an excited state, and D^+ and $F\bullet$ represent all the fragments created on ionization. Note that EI can be performed at low partial pressures, and in these experiments, the electron beam energy is modulated by the trapping potential applied to the inner ring electrode.

Chemical ionization (CI), a soft ionization technique, occurs at higher ion trap pressures ($>1 \times 10^{-6}$ torr) in the presence of an appropriate reagent (Field, 1968). One of the most common CI techniques is based on proton transfer. CI by proton transfer begins with EI of a neutral reagent molecule (RH), typically resulting in a radical cation (RH$^+\bullet$) (see Eq. 3 below). The radical cation is very reactive and can directly ionize a neutral sample molecule through charge exchange, or it can react with other reagents to produce more CI reagent ions. In the case of proton-transfer CI, the radical cation (RH$^+\bullet$) may react with another neutral reagent (RH) to yield a protonated reagent ion (RH$_2^+$), as shown in Eq. 4. A proton can then be transferred from the protonated reagent ion to a second neutral molecule (M) if the proton affinity (PA) of the target (M) is larger than that of the neutral reagent molecule (RH) (see Eq. 5). A simplified and generic proton transfer CI reaction scheme is

$$RH + e^- \rightarrow RH^{+\bullet} + 2e^- \qquad (3)$$

$$RH^{+\bullet} + RH \rightarrow RH_2^+ + R^\bullet \qquad (4)$$
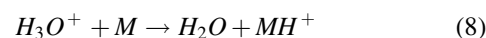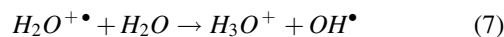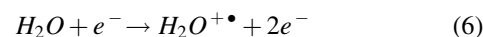
$$RH_2^+ + M \rightarrow RH + MH^+ \qquad (5)$$

It is possible for the target molecule to undergo EI even at higher trap pressures, though the likelihood is small due to

there being many more CI reagent molecules than target molecules and due to collisions with the CI reagent. Conversely, it is possible for CI to occur at low trap pressures, but it is not the dominant process as it is dependent on collisions.

For CI, the energy imparted to the sample molecule is dictated by the difference in PAs between the neutral reagent (RH) and sample molecule (M). A small difference in PAs between M and RH will typically result in ionization with little to no fragmentation. In this study, ionization by low-energy protonation with reagents and samples relevant to Ocean Worlds is the primary goal to avoid severe fragmentation. Water, acetonitrile, and acetone are compared as CI reagents and against EI. Table 1 includes the PAs of neutral molecules relevant to this study. Water, acetonitrile, and acetone are compared as CI reagents to probe the effect of ΔPA. For the experiments presented here, the CI reagent (*i.e.*, RH) is introduced either directly into the trap through the 1/16 in. tube (Fig. 1F) or through the sample line (Fig. 1E) as a small portion (1%/vol) of the sample solution.

Regardless of the CI reagent, water is present during these experiments, resulting in the production of hydronium ions (H_3O^+). The formation of hydronium in the presence of nitrogen has been previously studied (Good *et al.*, 1970). It is reasonable to expect hydronium formation to follow a scheme similar to that presented by Eqs. 3–5, especially when there is significantly more water present than nitrogen. It is possible to create higher-order water clusters (Good *et al.*, 1970); however, these clusters are not observed in the mass spectra presented here (see Supplementary Fig. S2 and the Discussion for more details). When no other reagent gases are present, hydronium then goes on to protonate the sample molecule. A reaction scheme is shown next.

$$H_2O + e^- \rightarrow H_2O^{+\bullet} + 2e^- \qquad (6)$$

$$H_2O^{+\bullet} + H_2O \rightarrow H_3O^+ + OH^\bullet \qquad (7)$$

$$H_3O^+ + M \rightarrow H_2O + MH^+ \qquad (8)$$

If acetonitrile or acetone is present at a sufficient abundance (*i.e.*, in the CI pressure regime, $>1 \times 10^{-6}$ torr), it is protonated by hydronium and, in turn, protonates the sample molecule. Acetonitrile and acetone will have analogous schemes, and the

TABLE 1. MOLECULAR WEIGHTS, ABBREVIATIONS, AND GAS-PHASE PROTON AFFINITIES OF NEUTRAL ORGANIC MOLECULES AND CHEMICAL IONIZATION REAGENTS

Molecule	Abbreviation	Molecular weight (amu)[a]	E_{pa} (kJ·mol^{-1})[a]
Lauric acid	LA	200.32	–
Glycine	*Gly*	75.07	886.5
Alanine	*Ala*	89.09	901.6
Serine	*Ser*	105.09	914.6
Methionine	*Met*	149.21	935.4
Phenylalanine	*Phe*	165.19	922.9
Water	—	18.02	691
Acetonitrile	—	41.05	779.2
Acetone	—	58.08	812

[a]Values obtained from the *CRC Handbook of Chemistry and Physics* (Rumble, 2018).
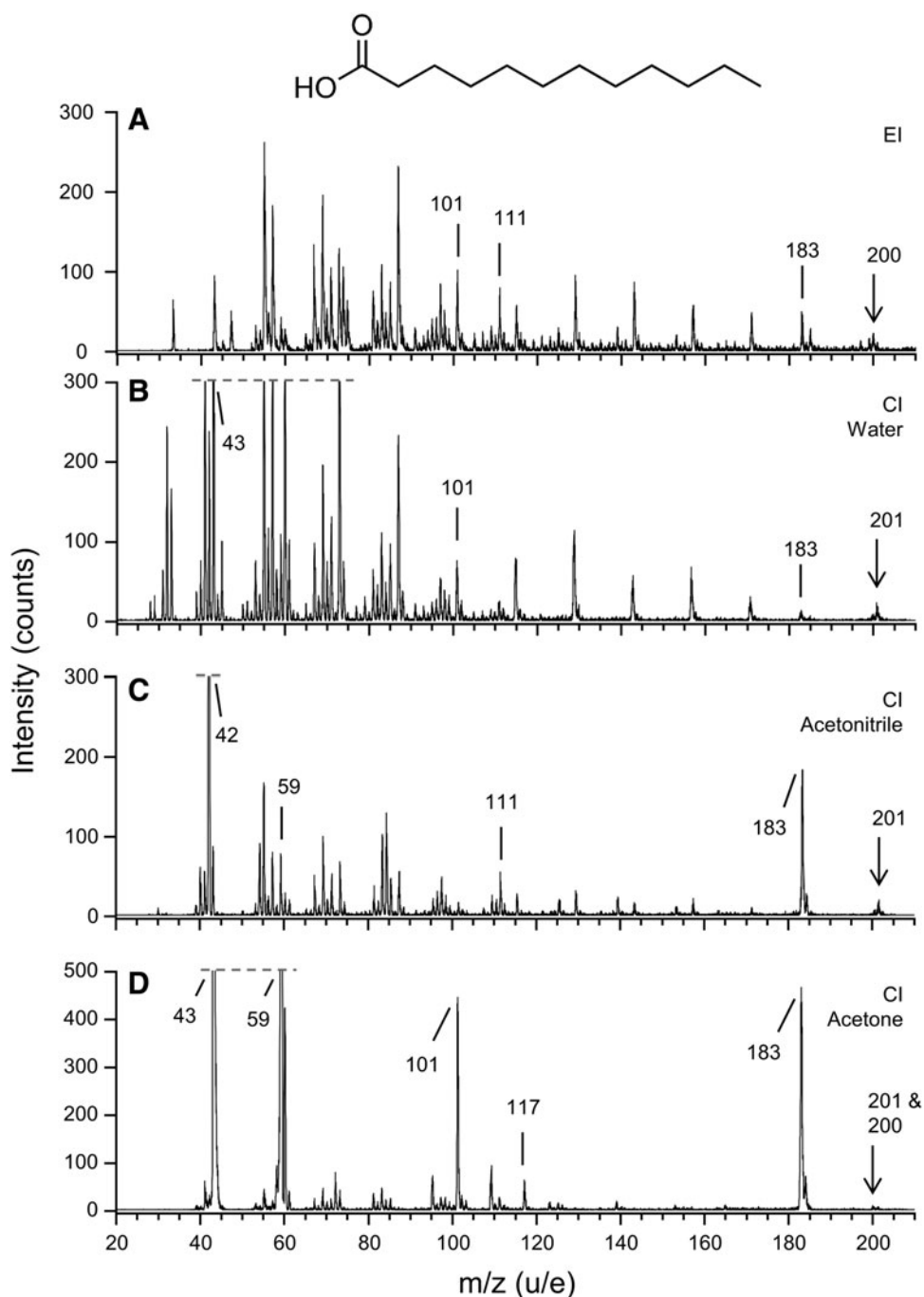
FIG. 2. Mass spectra of lauric acid collected by EI **(A)** and CI by using water **(B)**, acetonitrile **(C)**, and acetone **(D)**. The lauric acid structure is included above the EI spectrum. The parent ion and some high mass fragment *m/z*'s are labeled. Note that some peaks have been truncated as indicated by a dashed line.

reaction scheme once hydronium is formed (see Eq. 6 and 7 above) for acetonitrile (CH_3CN) is as follows:

$$H_3O^+ + CH_3CN \rightarrow H_2O + CH_3CNH^+ \qquad (9)$$

$$CH_3CNH^+ + M \rightarrow CH_3CN + MH^+ \qquad (10)$$
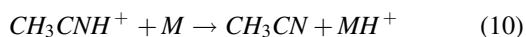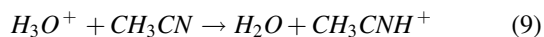
The gas-phase PAs of relevant AAs and CI reagents can be found in Table 1. As with most high-molecular-weight FAs, the PA of lauric acid (LA) is not known; however, it is rea-sonable to estimate the PA to be greater than or equal to propanoic acid (797.2 kJ·mol^{-1}), the largest unsaturated FA for which the PA is known (Rumble, 2018). This suggests that at most 150 kJ·mol^{-1} of energy will be imparted to LA on protonation with water. The energy difference is even greater when ionizing AAs. Glycine, the AA in this study with the lowest PA, will gain 196 kJ·mol^{-1} on ionization. Therefore, water CI is expected to induce fragmentation. To ''soften'' ionization with CI, a molecule with a larger PA than water (but a smaller PA than the sample) should be chosen. Here,

acetone (PA = 812 kJ·mol^{-1}) and acetonitrile (PA = 779.2 kJ·mol^{-1}) were chosen as our "soft" CI reagents, although any gas with a PA near 810 kJ·mol^{-1} would also work.

Solutions of 1 mg/mL (1000 ppm) LA were prepared by dissolving LA powder in acetonitrile and vortexing to ensure complete mixing. Acetonitrile was chosen as the solvent as it is better than water at dissolving nonpolar molecules (*e.g.*, FAs). AA mixture solutions comprising 0.2 mg/mL (200 ppm) each glycine (*Gly*), alanine (*Ala*), serine (*Ser*), methionine (*Met*), and phenylalanine (*Phe*) in 1/99%/vol. acetone/water were made in a similar fashion. A complete list of chemicals and a more detailed solution-making procedure can be found in Supplementary Table S1. Molecular weights of LA, the AAs, and CI reagents are included in Table 1.

3. Results

The differences in ionization technique can be observed in Fig. 2, which presents mass spectra of LA collected with EI (Fig. 2A) and CI with water (Fig. 2B), acetonitrile (Fig. 2C), and acetone (Fig. 2D). The LA peak is labeled with its *m/z*, 200 for LA$^+$• or 201 protonated LA (LAH$^+$), representing the radical cation or protonated parent ion, depending on which is present. To aid in the comparison of the mass spectra, the most intense peaks are truncated, as indicated by a dashed line. A direct comparison of the JPL EI spectrum and the National Institute for Standards and Technology (NIST) EI spectrum can be found in Supplementary Fig. S3.

Comparing the EI mass spectrum with the CI mass spectra highlights some expected differences. First, EI generally results in a larger number of low-mass fragments than CI, with the exception of water CI (see Fig. 2). Second, EI produces a radical cation parent species whereas CI produces protonated LA. Finally, CI yields the cleanest (and therefore easiest to interpret) mass spectrum (Fig. 2D). The main difference between the various CI reagents, all of which are introduced as "pure" reagents in the gas phase, is the extent of fragmentation. Water produces the most fragments followed by acetonitrile and then acetone.

The water CI mass spectrum is particularly congested at low mass (20–100 amu) and contains peaks that are not a product of LA fragmentation (see Supplementary Fig. S2 for a comparison of the JPL EI and water CI mass spectra). The intense 42 amu feature corresponds to protonated acetonitrile (CH$_3$CNH$^+$), which is known to fragment to 41, 40, and 39 amu (Stein, 2018). The presence of acetonitrile is likely a result of background carryover, as it is the solvent in the LA solutions deposited on the ion trap.

The low mass regions of the acetonitrile and acetone mass spectra contain fewer LA fragments. The acetonitrile mass spectrum contains two peaks that do not arise from LA, namely protonated acetonitrile and acetone (42 and 59 amu, respectively; Fig. 2C), with acetone arising from background carryover. The most intense peak is protonated acetonitrile (42 amu). The low mass acetone mass spectrum is the cleanest, with two intense peaks corresponding to protonated acetone (59 amu) and one of its fragments (43 amu).

The high mass range (101–210 amu) of the water CI mass spectrum is qualitatively similar to the EI spectrum for LA, except for the presence of the LA$^+$• (*m/z* 200) for EI-MS and the LAH$^+$ (*m/z* 201) for water CI-MS. In all of the CI mass spectra, LAH$^+$ is observed. The high mass region contains fewer frag-
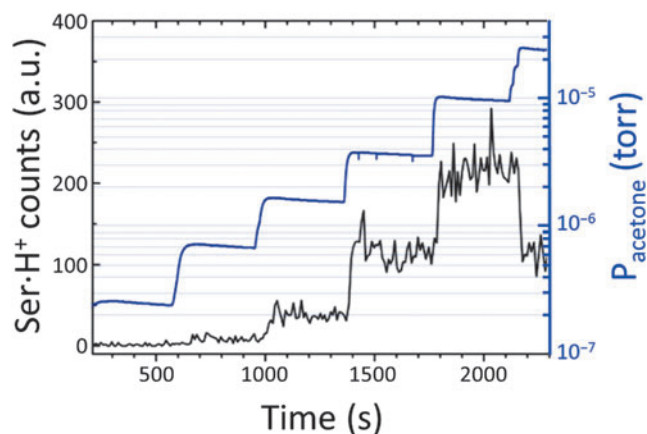

FIG. 3. Amount of *Ser*H$^+$ detected as a function of acetone pressure. The counts increase and reach a maximum at $\sim 1 \times 10^{-5}$ torr ($\sim 1 \times 10^{-5}$ mbar), above which there is a sharp decrease in signal. *Ser*H$^+$, protonated serine.

ments in the acetonitrile CI mass spectrum. Containing the same fragmentation peaks, the intensities of the 111 and 183 amu peaks are larger than observed with water CI whereas the other fragment intensities are diminished. Finally, the acetone mass spectrum is the cleanest of all. There are far fewer fragment peaks, with the fragments at *m/z* 101 and 183 dominating the higher mass region. LAH$^+$ fragments with *m/z* 101, 111, and 183 correspond to the loss of (CH$_2$)$_5$(CH$_3$)$_2$, (CH$_2$)$_3$(CH$_3$)$_2$ and H$_2$O, and H$_2$O, respectively, from LA. The protonated acetone dimer is observed at 117 amu.

For the AAs, the relationship between the amount of acetone introduced into the trap as a pure reagent gas and the amount of protonated serine (*Ser*H$^+$) detected is presented in Fig. 3. A significant amount of *Ser*H$^+$ is not detected until $\sim 2 \times 10^{-6}$ torr ($\sim 3 \times 10^{-6}$ mbar) of acetone has been introduced into the trap, which likely indicates a shift from EI- to CI-dominated ionization. The counts continue to increase with the pressure until $\sim 2 \times 10^{-5}$ torr, where there is a drastic decrease in signal intensity. A pressure of 1×10^{-5} torr yields the maximum counts and corresponds to a factor of 5.5 increase in signal compared with an acetone pressure of 2×10^{-7} torr. The sudden loss of counts is likely the result of increased collisions with neutral acetone in the trap (Nikolić *et al.*, 2015). These trends are expected to apply to all samples, including FAs.

Figure 4 presents the mass spectra of a mixture of five AAs produced from EI (top) and acetone CI (middle). The MS/MS mass spectrum of protonated methionine (150 amu) is presented in the bottom panel of Fig. 4. The AA solvent is mostly water with some acetone (1%/vol), and as such, the CI reagent is introduced as a dopant in the sample solution rather than as a gas as it was with LA. The protonated AA peaks are labeled with their *m/z*'s and color-coded (see Fig. 4 for more details). A CI spectrum with all major peaks labeled with *m/z*'s can be found in Supplementary Fig. S4, and Table 2 contains the protonated parent and ammonia- and formic acid-loss fragment masses.

As with LA, the low mass region of the EI mass spectrum is heavily congested, and the AA parent peaks have little to no intensity. Due to the congestion in the low-mass region, it is difficult to deconvolute the various AA fragments. A comparison of the EI mass spectrum and a compilation of
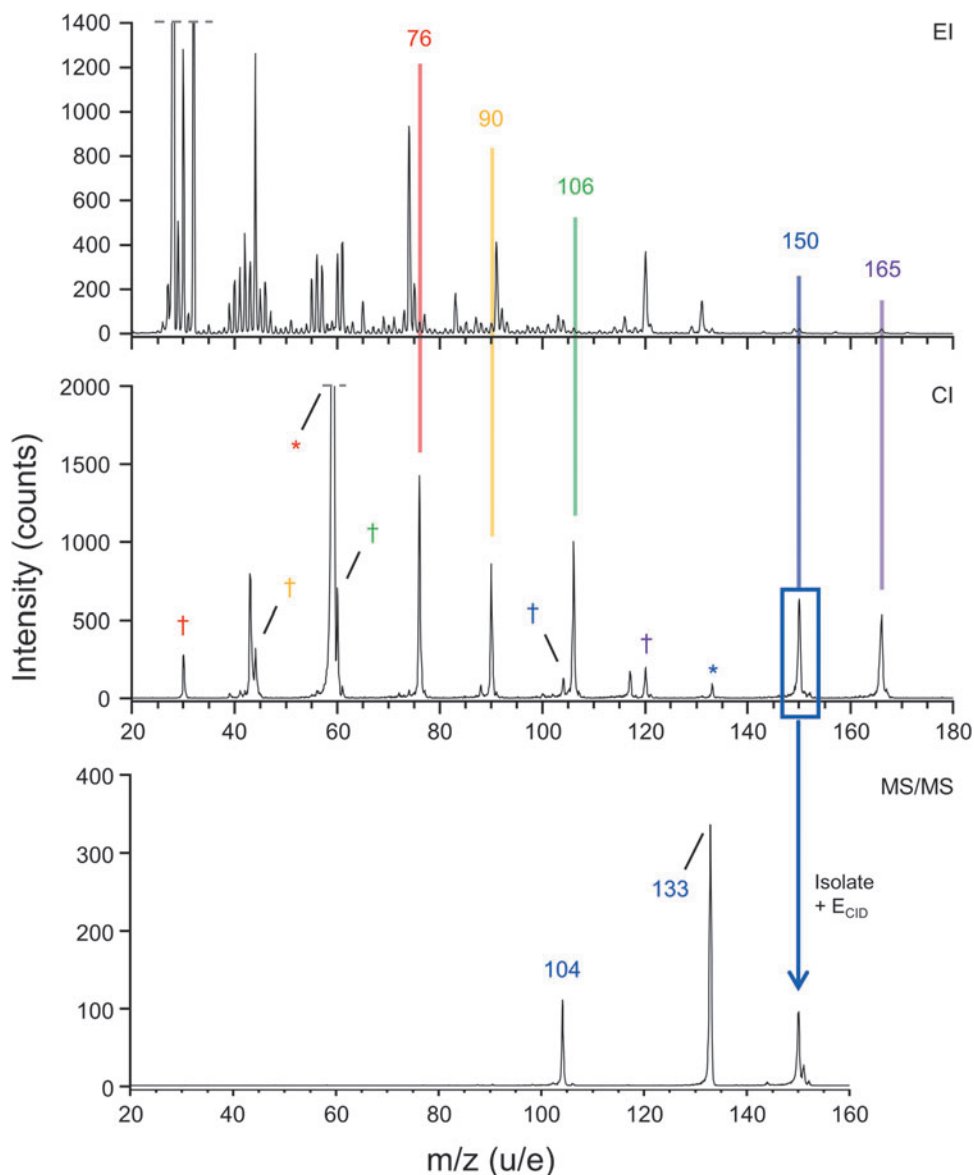
FIG. 4. Mass spectra of an amino acid mixture produced by EI (top), acetone CI (middle), and MS/MS of protonated methionine (bottom). The amino acids are color coded and labeled with their *m/z* ratios. Glycine and its fragments are labeled in red, alanine in orange, serine in green, methionine in blue, and phenylalanine in purple. Fragments corresponding to ammonia and formic acid loss are labeled with an asterisk (*) and dagger (†), respectively. Relevant *m/z*'s can be found in Table 2. Note that some peaks have been truncated as indicated by a dashed line. MS/MS, tandem mass spectrometry.

EI mass spectra for the AAs from NIST can be found in Supplementary Fig. S5. Overall, there is good qualitative agreement between the two EI mass spectra.

On the other hand, the CI mass spectrum is easily interpreted. All of the peaks can be readily assigned, and protonated AA peaks are more intense than their fragments. As seen earlier, protonated acetone (59 amu) is the most intense feature of the CI mass spectrum, and its dimer (117 amu) and fragment (43 amu) are also observed. Peaks consistent with formic acid loss from all AAs are observed and labeled with daggers (†). Only methionine definitively undergoes ammonia-loss as evidenced by the 133 amu feature. It is possible glycine also loses an ammonia; however, unambiguous assignment is not possible due to a mass degeneracy with protonated acetone (59 amu).

The MS/MS spectrum (Fig. 4 bottom) is less congested than either the EI or CI mass spectra. A protonated methionine peak (150 amu) is observed in addition to ammonia- and formic acid-loss fragments (133 and 104 amu, respectively). The MS/MS spectrum can be used as a "fingerprint" for more specific identification in the AA mixture CI mass spectrum. Note that water was used as the collision gas, which is directly relevant to measurements taken in an excess-water environment, such as one would expect on an Ocean World.

4. Discussion

The mass spectra of an FA, LA, and several AAs have been collected by introducing a liquid sample directly into a

TABLE 2. PROTONATED AMINO ACID MASSES AND
AMMONIA- AND FORMIC ACID-LOSS FRAGMENT MASSES

Amino acid	Mass (amu)	Observed
GlycineH⁺	76	Y
-NH₃	59	M
-HCOOH	30	Y
AlanineH⁺	90	Y
-NH₃	73	N
-HCOOH	44	Y
SerineH⁺	106	Y
-NH₃	89	N
-HCOOH	60	Y
MethionineH⁺	150	Y
-NH₃	133	Y
-HCOOH	104	Y
PhenylalanineH⁺	166	Y
-NH₃	149	M
-HCOOH	120	Y

The species observed in the chemical ionization mass spectrum in Figure 4 are indicated. M = maybe; N = no; Y = yes.

quadrupole ion trap. Two ionization techniques, EI and CI, are compared by the ease with which their mass spectra can be assigned. Generally, EI spectra are complicated with many peaks (particularly in the 20–100 amu range), as this method produces many fragments. The EI spectra of LA (Fig. 2A) and the AA mixture (Fig. 4 top panel) demonstrate this low-mass congestion, although almost every peak in the LA sample and the sample containing five AAs can be identified in the EI mass spectra (see Supplementary Figs. S2 and S5 for more detail). Samples with more molecules will generate increasingly congested low-mass regions when utilizing EI. If a technique is to be able to assign m/z ratios to molecular species, it is imperative to obtain "cleaner" mass spectra or employ other methods to assign their masses.

CI is generally considered a softer ionization technique than EI, but it can still yield spectra congested with many fragments. Three different CI reagents were tested to demonstrate "harder" and "softer" CI: water, acetonitrile, and acetone. The gas-phase PAs of each CI reagent and of LA and the AAs are listed in Table 1. The ordering of gas-phase PAs is thus: water < acetonitrile < acetone. The PA of LA is not known, as is the case with most of the FAs (Rumble, 2018). Regardless of the PA of LA, the CI energy ordering is water > acetonitrile > acetone.

The result of lowering the ΔPA is cleaner mass spectra, with acetone yielding the fewest fragments by m/z. This is exemplified in Fig. 2B–D. In Fig. 2D, both LA⁺• and LAH⁺ are observed in the acetone CI mass spectrum, which likely results from collisions of LAH⁺ with neutral gases in the trap to form LA⁺•. Figure 3 shows that introducing acetone into the trap is beneficial (i.e., increases the sample counts), but only to a maximum trap pressure of $\sim 2 \times 10^{-5}$ torr ($\sim 3 \times 10^{-5}$ mbar) where a sharp decrease in ion counts is observed.

Although acetone, a common CI reagent, was used here, another molecule with a similar PA could be used instead. In fact, a molecule with a lower molecular weight and similar PA is advantageous as collisions with heavier reagent gases can induce fragmentation and/or cause ions to be lost from the trap. An

example of a lighter molecule with a similar PA is cyclopropane with a molecular weight of 40 amu and a PA of 818.5 kJ·mol⁻¹. AA CI could be softened further by choosing a reagent with a PA closer to glycine (886.5 kJ·mol⁻¹), such as ammonia (17 amu; 853.6 kJ·mol⁻¹) and chloromethylene (48 amu; 874.1 kJ·mol⁻¹), though these would be unable to ionize the FAs.

Measurements of the cosmic dust analyzer (CDA) instrument aboard the Cassini spacecraft have observed hydrated hydronium ($H_3O^+(H_2O)_n$) and hydrated sodium ($Na^+(H_2O)_n$) clusters in Saturn's E ring and Enceladus' plumes (Hillier et al., 2007; Postberg et al., 2008, 2011). However, H_3O^+ was only observed in the water CI mass spectrum. The absence of peaks at 37, 55, 73, and 91 amu indicates that $H_3O^+(H_2O)_n$ clusters are not formed during our experiments (See Supplementary Fig. S3 for more details).

H_3O^+ is not observed in the other CI mass spectra because all of the hydronium formed is deprotonated by the CI reagent (i.e., acetonitrile or acetone). Hydronium is observed in the water CI mass spectrum because water is continuously introduced into the QITMS. However, even in this case, $H_3O^+(H_2O)_n$ clusters are not observed, which indicates that the QITMS operating settings are not conducive to water cluster formation.

Searching for biosignatures in an excess water environment presents several challenges. First, water CI yields mass spectra with many fragments, but the addition of a higher PA CI reagent, such as acetone, yields little fragmentation and/or intense protonated parent ions. Introducing a small amount of secondary CI reagent works only if the second reagent has a higher PA than water. In a flight-like scenario, one might consider introducing the vapor from a reservoir containing a water-acetone mixture that is isolated by a microvalve to soften ionization and obtain cleaner mass spectra. Introducing a vapor from a reservoir through a microvalve has flight heritage and was used to introduce calibrant gasses (Darrach et al., 2011; Madzunkov et al., 2018). Further, introducing water into the QITMS for sample analysis will help mitigate the effects of fluctuations in water pressure that one would expect while sampling Enceladus' plumes.

Since it is not necessarily the case that the best CI reagent for FAs is the same for AAs, including a second CI reagent-water reservoir for AAs on an in situ instrument could yield less AA parent ion fragmentation. The CI reagent for FAs will be capable of ionizing both the FAs and AAs present in the sample, whereas the AA CI reagent will only be able to ionize the AAs present. A flight instrument with two CI reagents might, therefore, include two reservoirs (one with an AA CI reagent-water mixture, the other with an FA CI reagent-water mixture) that are isolated with microvalves. Both reservoirs could be isolated from the QITMS, or one microvalve at a time could be opened to introduce either the AA or the FA CI reagent into the QITMS.

The ability to isolate one m/z and conduct MS/MS experiments is another advantage of the QITMS. The bottom panel of Fig. 4 exemplifies how MS/MS can aid in the interpretation of a mass spectrum containing multiple chemical compounds. By isolating a single m/z and fragmenting it, one obtains a fragmentation fingerprint and can pinpoint which of the peaks in the full MS are fragments of the original m/z. A library of biomarker fingerprints can be built to enable the assignment of even more complicated mixtures. Perhaps most importantly, it has been shown that

water, a species abundant on an Ocean World, can be used as a collision gas for MS/MS experiments.

The resolution of the QITMS [m/Δm(FWHM)] operating in boundary ejection mode is 750 at 320 amu and is 4000 at 64 amu for resonant ejection mode (Darrach et al., 2015), which indicates that we can easily resolve masses that differ by 1 amu. However, this resolution is not sufficient to resolve masses that differ by less than 1 amu. Further, the ability to determine whether there are constitutional isomers (i.e., molecules that have the same chemical formula but different connectivity) cannot be resolved by increasing the m/Δm. In these cases, MS/MS is a useful tool to identify isomers, as it might be possible to determine whether there are multiple species with the same m/z ratio (or m/z ratios that lie within 1 amu) by studying fragmentation patterns.

In theory, different structural isomers could fragment in unique ways. A fragmentation pattern that contains additional peaks or discrepancies in fragment intensities could indicate the presence of one or more isomers. For example, glycine (NH_2-CH_2-COOH) is known to lose COOH and NH_2CH_3 fragments, whereas acetohydroxamic acid (OH-NH-$COCH_3$) is known to produce H_2O- and HONH-loss fragments. In addition, we can build a fragmentation library for molecules that do not have known fragmentation patterns. A future study is planned to conduct MS/MS on a sample with an AA and multiple structural isomers, with the ultimate goal of quantifying the amount(s) of amino acid(s) and isomers present. The simplest AA, glycine, has 7 constitutional isomers and 98 molecules (either neutral or charged) have molecular weights between 74.5 and 75.5 amu. The number of isomers will increase nonlinearly as the AA/molecule grows in complexity. A method allowing for the disambiguation of a target molecule and its isomers is of great importance.

Several aspects of the experiments detailed here are directly applicable to an Ocean World mission wherein ice grains are sampled from a cryovolcanic plume. Of particular relevance is the soft CI ionization method and the introduction of a water/acetone mixture from a reservoir. On such a mission, an ice grain traveling at <5 km/s would strike the QITMS, resulting in the volatilization or impact ionization of compounds ensconced in the ice grain. Volatilized molecules can then be ionized by acetone CI and detected as described in this article.

Ions produced from impact ionization could also be detected by the MS, but further design considerations and lab testing would be necessary to ensure it. Generally, externally generated ions require additional ion guiding elements and a collision gas to be introduced into the QITMS for efficient trapping (McLuckey et al., 1994; Gross, 2011; Kamrath et al., 2011).

Molecular dissociation has been found to be unfavorable for hypervelocity impacts of bare hydrocarbons on a TiO_2 surface below 5 km/s (Jaramillo-Botero et al., 2012). Further, dissociative adsorption and scattering processes do not become favorable until ~6 km/s. Therefore, impacts of <5 km/s are predicted to only produce vibrationally and translationally excited molecules after impact. In the 2012 study by Jaramillo-Botero et al., they assumed that there were no collisions with background gas molecules after impact. The results of Jaramillo-Botero et al. have been used to inform the analysis of ion and neutral mass spectrometer (INMS) data (Waite et al., 2005, 2009).

It is reasonable to expect that the speed at which dissociation becomes favorable will be extended to higher speeds as the molecule is surrounded by more and more molecules (e.g., if it is ensconced in an ice grain). Further, collisions with a background gas will collisionally cool the vibrationally excited molecules, thus reducing fragmentation arising from predissociation. It is plausible that the CI reagent vapor can also act as the collision gas.

Molecules in the ice grain that undergo impact ionization (II) will fragment to varying degrees depending on the amount of energy imparted to the ion. As with CI, II can be classified as "hard" or "soft." Generally, more energy imparted to a molecule will result in more fragmentation. Increasing the pressure in the trap by introducing vapor from a water/acetone reservoir as demonstrated here can help reduce the fragmentation of vibrationally excited organic species via collisional cooling while having the simultaneous benefits of introducing a soft CI reagent and minimizing pressure fluctuations in the trap, which will inevitably occur during ice grain sampling.

The experiments presented here represent CI of volatilized compounds and MS/MS analysis on molecules that undergo soft II during ice grain sampling (i.e., molecules with impact velocities <5 km/s). The sampling and analysis of ions created by II is a topic that has already been explored (Postberg et al., 2009, 2018), and an instrument focusing on this regime, the surface dust analyzer (SUDA), has been selected for the Europa Clipper mission (Kempf et al., 2014).

There are many mass spectrometers with flight heritage that have been selected for flight missions. They utilize a variety of ionization techniques and have differing mass ranges, resolutions, sensitivities, weights, and power requirements. Table 3 compares some characteristics of six flight heritage/flight-selected mass spectrometers and the QITMS. There are many mass spectrometer characteristics of importance when determining which instrument is best for a mission, and each mass spectrometer has its strong suits and drawbacks.

The QITMS, similar to many other mass spectrometers listed here, utilizes EI. The resolution of the QITMS (750 for boundary ejection; 4000 for resonant ejection) is sufficiently high to confidently identify ions that differ by 1+ amu across the entire mass range. The QITMS has modest power requirements and is one of the lightest mass spectrometers currently developed. The ionization method presented here extends the capabilities of the QITMS to include the ability to use CI, which enables MS/MS and eases (and in some cases, enables) mass spectral analysis.

The identity of a chemical species can impose constraints on the technique presented here. In these studies, neutral molecules are introduced into the QITMS and are chemically ionized after they evaporate. However, it is possible for ions generated from neutral molecules on hypervelocity impact to be analyzed by the QITMS. Further, depending on the space environment, one might expect to sample ions, organics chelated with transition metals, or molecules with salty counter ions. The QITMS itself is independent with respect to the nature of the molecular or complexed species so long as it is in the gas phase (see the final Discussion paragraph for more on the QITMS sensitivity). However, some consideration is needed to ensure that ions created as a result of hypervelocity impact are efficiently trapped in the QITMS.

If the analyte molecule's PA is lower than the CI reagent's PA, those molecules will not be ionized via CI. This is one of the biggest drawbacks to CI, although explorations of Ocean Worlds mean that water will almost certainly be present, which

TABLE 3. COMPARISON OF MASS SPECTROMETERS WITH FLIGHT HERITAGE OR THAT HAVE BEEN SELECTED
FOR A MISSION AND THE JET PROPULSION LABORATORY QUADRUPOLE ION TRAP MASS SPECTROMETER

Instrument	Ionization type	MS type	Mass range (amu)	Resolution (m/Δm)	Sensitivity	Weight (kg)/power (W)
CDA[a]	II	TOF	1–200*	20–50	10^4 counts/s	17/12
SUDA[b]	II	TOF	1–250	200–250	—	5/–
INMS[c]	EI	QMA	1–99	100 @ 99	10^{-3} (counts·s^{-1})/(particle·cm^{-3})	10/23
MASPEX[d]	EI	TOF	1–1500	25,000 @ 150; 65 bounces	0.02 (counts·s^{-1})/(particle·cm^{-3})	8/50
SAM QMS[e]	EI	QMA	2–535	<1 U	10^{-3} (counts·s^{-1})/(particle·cm^{-3})	20/25
MOMA[f]	EI/LD	LIT	50–500/ 50–1000	≤1 U ≤2 U	10 ppb	12/82 12/65
QITMS[g]	EI	Paul trap	10–300	750 @ 320 4000 @ 64**	10^{13} counts/torr/s[†]	9.5/35

Note that the QITMS is not packaged or optimized for a flight mission. The QITMS metrics are based on the Spacecraft Atmosphere Monitoring technology demonstration instrument that is set to be launched to the International Space Station in 2019.
*Up to 8000 amu in extended mode with m/Δm <20.
**Based on laboratory measurements on a testbed (*i.e.*, nonflight) instrument.
[†]Based on laboratory measurements on a testbed (*i.e.*, nonflight) instrument with an atomic species.
[a]Srama *et al.* (2004).
[b]Kempf *et al.* (2014).
[c]Waite *et al.* (2004).
[d]Brockwell *et al.* (2016).
[e]Mahaffy *et al.* (2011, 2012).
[f]Goesmann *et al.* (2017).
[g]Madzunkov *et al.* (2018).
CDA = cosmic dust analyzer; EI = electron impact ionization; II = impact ionization; INMS = ion and neutral mass spectrometer; LD, laser desorption; LIT, linear ion trap; MASPEX = mass spectrometer for planetary exploration; MOMA = Mars organic molecule analyzer; QITMS = quadrupole ion trap mass spectrometer; QMA, quadrupole mass analyzer; SAM QMS = surface analysis at Mars quadrupole mass spectrometer; SUDA = surface dust analyzer; TOF, time-of-flight.

has a fairly low PA, making it likely that we will be able to chemically ionize most of the chemical species present. However, a CI reagent must be chosen with care, as a reagent with a PA that is too low will cause fragmentation and a PA that is too high will not result in ionization.

Thus, the CI reagent needs to be "fine tuned" based on the target molecule of interest. Another drawback to our CI technique is that we use acetone as a CI reagent. Acetone and acetonitrile are known to be present in interstellar ice (or their analogues) (Snyder *et al.*, 2002; Belloche *et al.*, 2008a, 2008b), thus introducing uncertainty whether these molecules are present at the target. Even though CI is the ionization method of choice, EI can still be conducted, which will reduce the uncertainty associated with the presence of these molecules.

The technique described here was intended to do several things: (1) determine whether CI is possible in the QITMS, (2) determine whether CI sufficiently softens ionization so MS/MS can be conducted, and (3) determine whether water (a molecule with great abundance on an Ocean World) can be used as a collision gas in MS/MS. The technique as described here is intended to provide a qualitative analysis of a sample. The sensitivity of the QITMS is $\sim 10^{13}$ counts/ torr/s (Avice *et al.*, 2019); however, that is for atomic species that do not fragment (*i.e.*, Kr, Xe) and that are already in the gas phase and ionized by EI. In this study, volatility of a molecule depends on its vapor pressure, which limits how many molecules we transfer to the gas phase. The sensitivity is also connected to fragmentation. As fragmentation and the number of fragments increases, the sensitivity is reduced.

The sensitivity of this technique toward AAs and FAs is anticipated to be roughly equal. Future studies will focus on exploring ways to quantize the organics present and on probing the sensitivity of the QITMS by using this technique (*i.e.*, conditions where a small fraction of molecules are disproportionally transferred into the gas phase and ionized by CI).

If this technique is to be used to identify biomarkers, quantization is a necessity as the comparison of the relative abundances of both AAs and FAs is required to differentiate between molecules produced from abiotic and biotic sources. Other future studies will explore the possibility of impact vaporization followed by CI in the QITMS with a new instrument that is currently under construction.

An MS-based instrument sent to investigate the plume of an Ocean World can be broken down into three main experimental steps: sampling, ionizing, and mass analysis. The soft CI technique reported here addresses the ionizing and, to some degree, the mass analysis aspects of this potential instrument. AA and FA ionization has been softened, thus reducing the complexity of the mass spectrum and enabling MS/MS.

Additional experiments exploring impact volatilization would probe the sampling aspect of the instrument. A laboratory-based instrument is currently being constructed and characterized that can generate hypervelocity ice grains doped with organics of interest. These ice grains will be collided with the QITMS, ionized with soft CI, and finally mass analyzed. By coupling together an instrument that generates hypervelocity ice grains and the QITMS, the performance of the QITMS to ionize and analyze impact vaporized molecules can be characterized. This would build a

strong case for a flight instrument that could search for organics in the plume of an Ocean World.

5. Conclusions

The mass spectra of an FA and a mixture of AAs, biomarkers of particular interest in the search for extraterrestrial life, were collected with a miniature QITMS developed at JPL. A liquid sample was directly introduced into the QITMS, which successfully transferred FAs and AAs into the gas phase for ionization and detection. Two ionization techniques, electron impact and CI, were compared, and CI with a high PA reagent (here acetone) was found to produce the cleanest mass spectra. Further, in environments with excess water, it is imperative to introduce a second CI reagent to reduce sample fragmentation, particularly of compounds with high PAs. Acetone was found to produce the fewest fragments for both LA and the AAs, whereas another CI reagent with a lower mass but similar PA should yield even fewer fragments.

The combination of direct sample introduction and acetone CI can produce enough ions to undergo MS/MS with water from the sample solution as the collision gas. MS/MS spectra aid in assigning the full range mass spectrum by yielding a fragmentation "fingerprint." Using water evaporated from the sample as the collision gas is particularly relevant for measurements on Ocean Worlds given the preponderance of water. Further, introducing a water-CI reagent mixture on a mission to an Ocean World is likely to reduce the effects of water pressure fluctuations that one expects while passing through a cryogenic plume.

Future studies are planned based on the results of these experiments. Studies focused on obtaining quantitative information about the organics present and to directly probe the sensitivity of this technique are currently underway. Additional experiments exploring impact volatilization followed by CI are also planned, and a laboratory-based instrument is currently being constructed that will enable these experiments to be conducted.

Acknowledgments

Author Disclosure Statement

No competing financial interests exist.

Supplementary Material

https://www.liebertpub.com/doi/suppl/10.1089/ast.2018.1961
Supplementary Data
Supplementary Figure S1
Supplementary Figure S2
Supplementary Figure S3
Supplementary Figure S4
Supplementary Figure S5
Supplementary Table S1

References

Anderson, J.D., Schubert, G., Jacobson, R.A., Lau, E.L., Moore, W.B., and Sjogren, W.L. (1998) Distribution of rock, metals, and ices in Callisto. *Science* 280:1573–1576.

Arvidson, R.E., Bonitz, R.G., Robinson, M.L., Carsten, J.L., Volpe, R.A., Trebi-Ollennu, A., Mellon, M.T., Chu, P.C., Davis, K.R., Wilson, J.J., Shaw, A.S., Greenberger, R.N., Siebach, K.L., Stein, T.C., Cull, S.C., Goetz, W., Morris, R.V., Ming, D.W., Keller, H.U., Lemmon, M.T., Sizemore, H.G., and Mehta, M. (2009) Results from the Mars Phoenix lander robotic arm experiment. *J Geophys Res Planets* 114, E00E02, doi:10.1029/2009JE003408.

Avice, G., Belousov, A., Farley, K.A., Madzunkov, S.M., Simcic, J., Nikolić, D., Darrach, M.R., and Sotin, C. (2019) High-precision measurements of krypton and xenon isotopes with a new static-mode quadrupole ion trap mass spectrometer. *J Anal At Spectrom* 34:104–117.

Ball, A.J., Garry, J.R.C., Lorenz, R.D., and Kerzhanovich, V.V. (2007) *Planetary Landers and Entry Probes*. Cambridge University Press, New York.

Balsiger, H., Altwegg, K., Bochsler, P., Eberhardt, P., Fischer, J., Graf, S., Jäckel, A., Kopp, E., Langer, U., Mildner, M., Müller, J., Riesen, T., Rubin, M., Scherer, S., Wurz, P., Wüthrich, S., Arijs, E., Delanoye, S., Keyser, J.D., Neefs, E., Nevejans, D., Rème, H., Aoustin, C., Mazelle, C., Mèdale, J.-L., Sauvaud, J.A., Berthelier, J.-J., Bertaux, J.-L., Duvet, L., Illiano, J.-M., Fuselier, S.A., Ghielmetti, A.G., Magoncelli, T., Shelley, E.G., Korth, A., Heerlein, K., Lauche, H., Livi, S., Loose, A., Mall, U., Wilken, B., Gliem, F., Fiethe, B., Gombosi, T.I., Block, B., Carignan, G.R., Fisk, L.A., Waite, J.H., Young, D.T., and Wollnik, H. (2007) ROSINA–Rosetta orbiter spectrometer for ion and neutral analysis. *Space Sci Rev* 128:745–801.

Belloche, A., Menten, K.M., Comito, C., Müller, H.S.P., Schilke, P., Ott, J., Thorwirth, S., and Hieret, C. (2008a) Detection of amino acetonitrile in Sgr B2(N). *Astron Astrophys* 482:179–196.

Belloche, A., Menten, K.M., Comito, C., Müller, H.S.P., Schilke, P., Ott, J., Thorwirth, S., and Hieret, C. (2008b) Erratum to detection of amino acetonitrile in Sgr B2(N). *Astron Astrophys* 492:769–773.

Bleakney, W. (1930) The ionization of hydrogen by single electron impact. *Phys Rev* 35:1180–1186.

Bouquet, A., Mousis, O., Waite, J.H., and Picaud, S. (2015) Possible evidence for a methane source in Enceladus' ocean. *Geophys Res Lett* 42:1334–1339.

Brockwell, T.G., Meech, K.J., Pickens, K., Waite, J.H., Miller, G., Roberts, J., Lunine, J.I., and Wilson, P. (2016) The mass spectrometer for planetary exploration (MAXPEX). In *2016 IEEE Aerospace Conference*. March 5–12; Big Sky, MT.

Capaccioni, F., Coradini, A., Filacchione, G., Erard, S., Arnold, G., Drossart, P., De Sanctis, M.C., Bockelee-Morvan, D., Capria, M.T., Tosi, F., Leyrat, C., Schmitt, B., Quirico, E., Cerroni, P., Mennella, V., Raponi, A., Ciarniello, M., McCord, T., Moroz, L., Palomba, E., Ammannito, E., Barucci, M.A., Bellucci, G., Benkhoff, J., Bibring, J.P., Blanco, A., Blecka, M., Carlson, R., Carsenty, U., Colangeli, L., Combes, M., Combi, M., Crovisier, J., Encrenaz, T., Federico, C., Fink, U., Fonti, S., Ip, W.H., Irwin, P., Jaumann, R., Kuehrt, E., Langevin, Y., Magni, G., Mottola, S., Orofino, V., Palumbo, P., Piccioni, G., Schade, U., Taylor, F., Tiphene, D., Tozzi, G.P., Beck, P., Biver, N., Bonal, L., Combe, J.-P., Despan, D., Flamini, E., Fornasier, S., Frigeri, A., Grassi, D., Gudipati, M., Longobardo, A., Markus, K., Merlin, F., Orosei, R., Rinaldi, G., Stephan, K., Cartacci, M., Cicchetti, A., Giuppi, S., Hello,

Y., Henry, F., Jacquinod, S., Noschese, R., Peter, G., Politi, R., Reess, J.M., and Semery, A. (2015) The organic-rich surface of comet 67P/Churyumov-Gerasimenko as seen by VIRTIS/Rosetta. *Science* 347:aaa0628.

Choblet, G., Tobie, G., Sotin, C., Běhounková, M., Čadek, O., Postberg, F., and Souček, O. (2017) Powering prolonged hydrothermal activity inside Enceladus. *Nat Astron* 1:841–847.

Creamer, J.S., Mora, M.F., and Willis, P.A. (2017) Enhanced resolution of chiral amino acids with capillary electrophoresis for biosignature detection in extraterrestrial samples. *Anal Chem* 89:1329–1337.

Darrach, M.R., Chutjian, A., Bornstein, B.J., Croonquist, A.P., Garkanian, V., Haemmerle, V.R., Heinrichs, W.M., Karmon, D., Kenny, J., and Kidd, R.D. (2010) Validation test results from the vehicle cabin atmosphere monitor. In *40th Internation Conference on Environmental Systems*. July 11–15; Barcelona, Spain.

Darrach, M.R., Chutjian, A., Bornstein, B.J., Croonquist, A.P., Garkanian, V., Haemmerle, V.R., Heinrichs, W.M., Hofman, J., Karmon, D., Kenny, J., Kidd, R., Lee, S., MacAskill, J.A., Madzunkov, S., Mandrake, L., Schaefer, R., Rust, T., Thomas, J., and Toomarian, N. (2011) On-orbit measurements of the ISS atmosphere by the vehicle cabin atmosphere monitor. In *41st International Conferene on Enironmental Systems*. July 17–21; Portland, OR.

Darrach, M., Madzunkov, S., Schaefer, R., Nikolić, D., Simcic, J., Kidd, R., Neidholdt, E., Pilinski, M., Jaramillo-Botero, A., and Farley, K. (2015) The mass analyzer for real-time investigation of neutrals at Europa (MARINE). In *2015 IEEE Aerospace Conference*. March 7–14, 2015; Big Sky, MT. doi: 10.1109/AERO.2015.7119017

Domagal-Goldman, S.D., Wright, K.E., Adamala, K., Arina de la Rubia, L., Bond, J., Dartnell, L.R., Goldman, A.D., Lynch, K., Naud, M.-E., Paulino-Lima, I.G., Singer, K., Walter-Antonio, M., Abrevaya, X.C., Anderson, R., Arney, G., Atri, D., Azúa-Bustos, A., Bowman, J.S., Brazelton, W.J., Brennecka, G.A., Carns, R., Chopra, A., Colangelo-Lillis, J., Crockett, C.J., DeMarines, J., Frank, E.A., Frantz, C., de la Fuente, E., Galante, D., Glass, J., Gleeson, D., Glein, C.R., Goldblatt, C., Horak, R., Horodyskyj, L., Kaçar, B., Keresztari, A., Knowles, E., Mayeur, P., McGlynn, S., Miguel, Y., Montgomery, M., Neish, C., Noack, L., Rugheimer, S., Stüeken, E.E., Tamez-Hidalgo, P., Walker, S.I., and Wong, T. (2016) The astrobiology primer v2.0. *Astrobiology* 16:561–653.

Encrenaz, T. (2008) Remote sensing analysis of solar-system objects. *Physica Scripta* 130:id.014037.

Field, F.H. (1968) Chemical ionization mass spectrometry. *Acc Chem Res* 1:42–49.

Fortes, A.D. (2012) Titan's internal structure and the evolutionary consequences. *Planet Space Sci* 60:10–17.

Fulchignoni, M., Ferri, F., Angrilli, F., Ball, A.J., Bar-Nun, A., Barucci, M.A., Bettanini, C., Bianchini, G., Borucki, W., Colombatti, G., Coradini, M., Coustenis, A., Debei, S., Falkner, P., Fanti, G., Flamini, E., Gaborit, V., Grard, R., Hamelin, M., Harri, A.M., Hathi, B., Jernej, I., Leese, M.R., Lehto, A., Lion Stoppato, P.F., López-Moreno, J.J., Mäkinen, T., McDonnell, J.A.M., McKay, C.P., Molina-Cuberos, G., Neubauer, F.M., Pirronello, V., Rodrigo, R., Saggin, B., Schwingenschuh, K., Seiff, A., Simões, F., Svedhem, H., Tokano, T., Towner, M.C., Trautner, R., Withers, P., and Zarnecki, J.C. (2005) In situ measurements of the physical characteristics of Titan's environment. *Nature* 438:785–791.

Gao, Y. and Chien, S. (2017) Review on space robotics: toward top-level science through space exploration. *Sci Robot* 2:eaan5074.

Goesmann, F., Brinckerhoff, W.B., Raulin, F., Goetz, W., Danell, R.M., Getty, S.A., Siljeström, S., Mißbach, H., Steininger, H., Arevalo, R.D.J., Buch, A., Freissinet, C., Grubisic, A., Meierhenrich, U.J., Pinnick, V.T., Stalport, F., Szopa, C., Vago, J.L., Lindner, R., Schulte, M.D., Brucato, J.R., Glavin, D.P., Grand, N., Li, X., van Amerom, F.H.W., and Team T.M.S. (2017) The Mars organic molecule analyzer (MOMA) instrument: characterization of organic material in martian sediments. *Astrobiology* 17:655–685.

Good, A., Durden, D.A., and Kebarle, P. (1970) Ion–molecule reactions in pure nitrogen and nitrogen containing traces of water at total pressures 0.5–4 torr. Kinetics of clustering reactions forming $H^+(H_2O)_n$. *J Chem Phys* 52:212–221.

Gross, J.H. (2011) *Mass Spectrometry: A Textbook*. Springer, New York.

Grotzinger, J.P., Crisp, J., Vasavada, A.R., Anderson, R.C., Baker, C.J., Barry, R., Blake, D.F., Conrad, P., Edgett, K.S., Ferdowski, B., Gellert, R., Gilbert, J.B., Golombek, M., Gómez-Elvira, J., Hassler, D.M., Jandura, L., Litvak, M., Mahaffy, P., Maki, J., Meyer, M., Malin, M.C., Mitrofanov, I., Simmonds, J.J., Vaniman, D., Welch, R.V., and Wiens, R.C. (2012) Mars science laboratory mission and science investigation. *Space Sci Rev* 170:5–56.

Hand, E. (2008) Phoenix lander tastes its first ice. *Nature* doi: 10.1038/news.2008.1002.

Hand, K.P., Murray, A.E., Garvin, J.B., Brickerhoff, W.B., Christner, B.C., Edgett, K.S., Ehlmann, B.L., German, C.R., Hayes, A.G., Hoehler, T.M., Horst, S.M., Lunine, J.I., Nealson, K.H., Paranicas, C., Schmidt, B.E., Smith, D.E., Rhoden, A.R., Russell, M.J., Templeton, A.S., Willis, P.A., Yingst, R.A., Phillips, C.B., Cable, M.L., Craft, K.L., Hofmann, A.E., Nordheim, T.A., Pappalardo, R.P., and Team t.P.E. (2017) Report of the Europa Lander Science Definition Team. https://bizwhiznetwork.com/science-report-on-nasas-europa-lander-concept-released/

Hillier, J.K., Green, S.F., McBride, N., Schwanethal, J.P., Postberg, F., Srama, R., Kempf, S., Moragas-Klostermeyer, G., McDonnell, J.A.M., and Grün, E. (2007) The composition of Saturn's E ring. *Mon Not R Astron Soc* 377:1588–1596.

Hsu, H.-W., Postberg, F., Sekine, Y., Shibuya, T., Kempf, S., Horányi, M., Juhász, A., Altobelli, N., Suzuki, K., Masaki, Y., Kuwatani, T., Tachibana, S., Sirono, S.-i., Moragas-Klostermeyer, G., and Srama, R. (2015) Ongoing hydrothermal activities within Enceladus. *Nature* 519:207–210.

Jaramillo-Botero, A., An, Q., Cheng, M.-J., Goddard, W.A., Beegle, L.W., and Hodyss, R. (2012) Hypervelocity impact effect of molecules from Enceladus' plume and Titan's upper atmosphere on NASA's Cassini spectrometer from reactive dynamics simulation. *Phys Rev Lett* 109:213201.

Jia, X., Kivelson, M.G., Khurana, K.K., and Kurth, W.S. (2018) Evidence of a plume on Europa from Galileo magnetic and plasma wave signatures. *Nat Astron* 2:459–464.

Johnson, S.S., Anslyn, E.V., Graham, H.V., Mahaffy, P.R., and Ellington, A.D. (2018) Fingerprinting non-terran biosignatures. *Astrobiology* 18:915–922.

Kamrath, M.Z., Relph, R.A., Guasco, T.L., Leavitt, C.M., and Johnson, M.A. (2011) Vibrational predissociation spectroscopy of the H_2-tagged mono- and dicarboxylate anions of dodecanedioic acid. *Int J Mass Spectrom* 300:91–98.

Kempf, S., Altobelli, N., Briois, C., Grun, E., Horanyi, M., Postberg, F., Schmidt, J., Srama, R., Sternovsky, Z., Tobie, G., and Zolotov, M. (2014) SUDA: a dust mass spectrometer for compositional surface mapping for a mission to Europa

[abstract #EPSC2014-229]. In *2014 European Planetary Science Congress*. September 7–12; Cascais, Portugal.

Kivelson, M.G., Khurana, K.K., and Volwerk, M. (2002) The permanent and inductive magnetic moments of Ganymede. *Icarus* 157:507–522.

Leshin, L.A., Mahaffy, P.R., Webster, C.R., Cabane, M., Coll, P., Conrad, P.G., Archer, P.D., Atreya, S.K., Brunner, A.E., Buch, A., Eigenbrode, J.L., Flesch, G.J., Franz, H.B., Freissinet, C., Glavin, D.P., McAdam, A.C., Miller, K.E., Ming, D.W., Morris, R.V., Navarro-Gonzalez, R., Niles, P.B., Owen, T., Pepin, R.O., Squyres, S., Steele, A., Stern, J.C., Summons, R.E., Sumner, D.Y., Sutter, B., Szopa, C., Teinturier, S., Trainer, M.G., Wray, J.J., Grotzinger, J.P., Kemppinen, O., Bridges, N., Johnson, J.R., Minitti, M., Cremers, D., Bell, J.F., Edgar, L., Farmer, J., Godber, A., Wadhwa, M., Wellington, D., McEwan, I., Newman, C., Richardson, M., Charpentier, A., Peret, L., King, P., Blank, J., Weigle, G., Schmidt, M., Li, S., Milliken, R., Robertson, K., Sun, V., Baker, M., Edwards, C., Ehlmann, B., Farley, K., Griffes, J., Miller, H., Newcombe, M., Pilorget, C., Rice, M., Siebach, K., Stack, K., Stolper, E., Brunet, C., Hipkin, V., Leveille, R., Marchand, G., Sanchez, P.S., Favot, L., Cody, G., Fluckiger, L., Lees, D., Nefian, A., Martin, M., Gailhanou, M., Westall, F., Israel, G., Agard, C., Baroukh, J., Donny, C., Gaboriaud, A., Guillemot, P., Lafaille, V., Lorigny, E., Paillet, A., Perez, R., Saccoccio, M., Yana, C., Armiens-Aparicio, C., Rodriguez, J.C., Blazquez, I.C., Gomez, F.G., Gomez-Elvira, J., Hettrich, S., Malvitte, A.L., Jimenez, M.M., Martinez-Frias, J., Martin-Soler, J., Martin-Torres, F.J., Jurado, A.M., Mora-Sotomayor, L., Caro, G.M., Lopez, S.N., Peinado-Gonzalez, V., Pla-Garcia, J., Manfredi, J.A.R., Romeral-Planello, J.J., Fuentes, S.A.S., Martinez, E.S., Redondo, J.T., Urqui-O'Callaghan, R., Mier, M.P.Z., Chipera, S., Lacour, J.L., Mauchien, P., Sirven, J.B., Manning, H., Fairen, A., Hayes, A., Joseph, J., Sullivan, R., Thomas, P., Dupont, A., Lundberg, A., Melikechi, N., Mezzacappa, A., DeMarines, J., Grinspoon, D., Reitz, G., Prats, B., Atlaskin, E., Genzer, M., Harri, A.M., Haukka, H., Kahanpaa, H., Kauhanen, J., Kemppinen, O., Paton, M., Polkko, J., Schmidt, W., Siili, T., Fabre, C., Wilhelm, M.B., Poitrasson, F., Patel, K., Gorevan, S., Indyk, S., Paulsen, G., Gupta, S., Bish, D., Schieber, J., Gondet, B., Langevin, Y., Geffroy, C., Baratoux, D., Berger, G., Cros, A., d'Uston, C., Forni, O., Gasnault, O., Lasue, J., Lee, Q.M., Maurice, S., Meslin, P.Y., Pallier, E., Parot, Y., Pinet, P., Schroder, S., Toplis, M., Lewin, E., Brunner, W., Heydari, E., Achilles, C., Oehler, D., Coscia, D., Israel, G., Dromart, G., Robert, F., Sautter, V., Le Mouelic, S., Mangold, N., Nachon, M., Stalport, F., Francois, P., Raulin, F., Cameron, J., Clegg, S., Cousin, A., DeLapp, D., Dingler, R., Jackson, R.S., Johnstone, S., Lanza, N., Little, C., Nelson, T., Wiens, R.C., Williams, R.B., Jones, A., Kirkland, L., Treiman, A., Baker, B., Cantor, B., Caplinger, M., Davis, S., Duston, B., Edgett, K., Fay, D., Hardgrove, C., Harker, D., Herrera, P., Jensen, E., Kennedy, M.R., Krezoski, G., Krysak, D., Lipkaman, L., Malin, M., McCartney, E., McNair, S., Nixon, B., Posiolova, L., Ravine, M., Salamon, A., Saper, L., Stoiber, K., Supulver, K., Van Beek, J., Van Beek, T., Zimdar, R., French, K.L., Iagnemma, K., Goesmann, F., Goetz, W., Hviid, S., Johnson, M., Lefavor, M., Lyness, E., Breves, E., Dyar, M.D., Fassett, C., Blake, D.F., Bristow, T., DesMarais, D., Edwards, L., Haberle, R., Hoehler, T., Hollingsworth, J., Kahre, M., Keely, L., McKay, C., Wilhelm, M.B., Bleacher, L., Brinckerhoff, W., Choi, D., Dworkin, J.P., Floyd, M., Garvin, J., Harpold, D., Jones, A., Martin, D.K., Pavlov, A., Raaen, E., Smith, M.D., Tan, F., Meyer, M., Posner, A., Voytek, M., Anderson, R.C., Aubrey, A., Beegle, L.W., Behar, A., Blaney, D., Brinza, D., Calef, F., Christensen, L.,

Crisp, J.A., DeFlores, L., Ehlmann, B., Feldman, J., Feldman, S., Hurowitz, J., Jun, I., Keymeulen, D., Maki, J., Mischna, M., Morookian, J.M., Parker, T., Pavri, B., Schoppers, M., Sengstacken, A., Simmonds, J.J., Spanovich, N., Juarez, M.d.l.T., Vasavada, A.R., Yen, A., Cucinotta, F., Jones, J.H., Rampe, E., Nolan, T., Fisk, M., Radziemski, L., Barraclough, B., Bender, S., Berman, D., Dobrea, E.N., Tokar, R., Vaniman, D., Williams, R.M.E., Yingst, A., Lewis, K., Cleghorn, T., Huntress, W., Manhes, G., Hudgins, J., Olson, T., Stewart, N., Sarrazin, P., Grant, J., Vicenzi, E., Wilson, S.A., Bullock, M., Ehresmann, B., Hamilton, V., Hassler, D., Peterson, J., Rafkin, S., Zeitlin, C., Fedosov, F., Golovin, D., Karpushkina, N., Kozyrev, A., Litvak, M., Malakhov, A., Mitrofanov, I., Mokrousov, M., Nikiforov, S., Prokhorov, V., Sanin, A., Tretyakov, V., Varenikov, A., Vostrukhin, A., Kuzmin, R., Clark, B., Wolff, M., McLennan, S., Botta, O., Drake, D., Bean, K., Lemmon, M., Schwenzer, S.P., Anderson, R.B., Herkenhoff, K., Lee, E.M., Sucharski, R., Hernandez, M.A.d.P., Avalos, J.J.B., Ramos, M., Kim, M.H., Malespin, C., Plante, I., Muller, J.P., Ewing, R., Boynton, W., Downs, R., Fitzgibbon, M., Harshman, K., Morrison, S., Dietrich, W., Kortmann, O., Palucis, M., Williams, A., Lugmair, G., Wilson, M.A., Rubin, D., Jakosky, B., Balic-Zunic, T., Frydenvang, J., Jensen, J.K., Kinch, K., Koefoed, A., Madsen, M.B., Stipp, S.L.S., Boyd, N., Campbell, J.L., Gellert, R., Perrett, G., Pradler, I., VanBommel, S., Jacob, S., Rowland, S., Atlaskin, E., Savijarvi, H., Boehm, E., Bottcher, S., Burmeister, S., Guo, J., Kohler, J., Garcia, C.M., Mueller-Mellin, R., Wimmer-Schweingruber, R., Bridges, J.C., McConnochie, T., Benna, M., Bower, H., Blau, H., Boucher, T., Carmosino, M., Elliott, H., Halleaux, D., Renno, N., Wong, M., Elliott, B., Spray, J., Thompson, L., Gordon, S., Newsom, H., Ollila, A., Williams, J., Vasconcelos, P., Bentz, J., Nealson, K., Popa, R., Kah, L.C., Moersch, J., Tate, C., Day, M., Kocurek, G., Hallet, B., Sletten, R., Francis, R., McCullough, E., Cloutis, E., ten Kate, I.L., Kuzmin, R., Arvidson, R., Fraeman, A., Scholes, D., Slavney, S., Stein, T., Ward, J., Berger, J., and Moores, J.E. (2013) Volatile, isotope, and organic analysis of martian fines with the Mars Curiosity rover. *Science* 341:1238937.

Lorenz, R.D. (2016) Europa ocean sampling by plume fly-through: astrobiological expectations. *Icarus* 267:217–219.

Lunine, J.I. (2017) Ocean worlds exploration. *Acta Astronaut* 131:123–130.

Madzunkov, S. and Nikolić, D. (2014) Accurate Xe isotope measurement using JPL ion trap. *J Am Soc Mass Spectrom* 25:1841–1852.

Madzunkov, S.M., Schowalter, S., Nikolić, D., Diaz, E., Simcic, J., Kidd, R.D., White, V., Bae, B., Gill, J., Cisneros, I., *et al.* (2018) Progress report on the spacecraft atmosphere monitor's development model [abstract #ICES-2018-325]. In *48th International Conference on Environmental Systems*. July 8–12; Albuquerque, NM.

Mahaffy, P.R., Trainer, M.G., Eigenbrode, J.L., Franz, H.B., Stern, J.C., Harpold, D.N., Conrad, P.G., Raaen, E., and Lyness, E. (2011) Calibration of the quadrupole mass spectrometer of the sample analysis at Mars instrument suite [abstract #1556]. In *42nd Lunar and Planetary Science Conference*. March 7–11; Houston, TX.

Mahaffy, P.R., Webster, C.R., Cabane, M., Conrad, P.G., Coll, P., Atreya, S.K., Arvey, R., Barciniak, M., Benna, M., Bleacher, L., Brinckerhoff, W.B., Eigenbrode, J.L., Carignan, D., Cascia, M., Chalmers, R.A., Dworkin, J.P., Errigo, T., Everson, P., Franz, H., Farley, R., Feng, S., Frazier, G., Freissinet, C., Glavin, D.P., Harpold, D.N., Hawk, D., Holmes, V., Johnson, C.S., Jones, A., Jordan, P., Kellogg, J., Lewis, J., Lyness, E.,

Malespin, C.A., Martin, D.K., Maurer, J., McAdam, A.C., McLennan, D., Nolan, T.J., Noriega, M., Pavlov, A.A., Prats, B., Raaen, E., Sheinman, O., Sheppard, D., Smith, J., Stern, J.C., Tan, F., Trainer, M., Ming, D.W., Morris, R.V., Jones, J., Gundersen, C., Steele, A., Wray, J., Botta, O., Leshin, L.A., Owen, T., Battel, S., Jakosky, B.M., Manning, H., Squyres, S., Navarro-González, R., McKay, C.P., Raulin, F., Sternberg, R., Buch, A., Sorensen, P., Kline-Schoder, R., Coscia, D., Szopa, C., Teinturier, S., Baffes, C., Feldman, J., Flesch, G., Forouhar, S., Garcia, R., Keymeulen, D., Woodward, S., Block, B.P., Arnett, K., Miller, R., Edmonson, C., Gorevan, S., and Mumm, E. (2012) The sample analysis at Mars investigation and instrument suite. *Space Sci Rev* 170:401–478.

March, R.E. (1997) An introduction to quadrupole ion trap mass spectrometry. *J Mass Spectrom* 32:351–369.

McKay, C.P., Anbar, A.D., Porco, C., and Tsou, P. (2014) Follow the plume: the habitability of Enceladus. *Astrobiology* 14:352–355.

McLuckey, S.A., Van Berkel, G.J., Goeringer, D.E., and Glish, G.L. (1994) Ion trap mass spectrometry of externally generated ions. *Anal Chem* 66:689A–696A.

Neish, C.D., Lorenz, R.D., Turtle, E.P., Barnes, J.W., Trainer, M.G., Stiles, B., Kirk, R., Hibbitts, C.A., and Malaska, M.J. (2018) Strategies for detecting biological molecules on Titan. *Astrobiology* 18:571–585.

Niemann, H.B., Atreya, S.K., Bauer, S.J., Carignan, G.R., Demick, J.E., Frost, R.L., Gautier, D., Haberman, J.A., Harpold, D.N., Hunten, D.M., Israel, G., Lunine, J.I., Kasprzak, W.T., Owen, T.C., Paulkovich, M., Raulin, F., Raaen, E., and Way, S.H. (2005) The abundances of constituents of Titan's atmosphere from the GCMS instrument on the Huygens probe. *Nature* 438:779–784.

Nikolić, D., Madzunkov, S.M., and Darrach, M.R. (2015) Computer modeling of an ion trap mass analyzer, part I: low pressure regime. *J Am Soc Mass Spectrom* 26:2115–2124.

Norwood, J., Hammel, H., Milam, S., Stansberry, J., Lunine, J., Chanover, N., Hines, D., Sonneborn, G., Tiscareno, M., Brown, M., and Ferruit, P. (2016) Solar system observations with the James Webb space telescope. *Publ Astron Soc Pac* 128: 025004.

Paul, W. (1990) Electromagnetic traps for charged and neutral particles (nobel lecture). *Angew Chem Int Ed Engl* 29:739–748.

Poncy, J., Grasset, O., Martinot, V., and Gabriel, G. (2008) Preliminary assessment of a Ceres polar lander mission. In *European Planetary Science Congress 2008*. September 21–25; Münster, Germany.

Porco, C.C., Helfenstein, P., Thomas, P.C., Ingersoll, A.P., Wisdom, J., West, R., Neukum, G., Denk, T., Wagner, R., Roatsch, T., Turtle, E., McEwen, A., Johnson, T.V., Rathbun, J., Veverka, J., Wilson, D., Perry, J., Spitale, J., Brahic, A., Burns, J.A., Del Genio, A.D., Dones, L., Murray, C.D., and Squyres, S. (2006) Cassini observes the active south pole of Enceladus. *Science* 311:1393–1401.

Porco, C.C., Dones, L., and Mitchell, C. (2017) Could it be snowing microbes on Enceladus? Assessing conditions in its plume and implications for future missions. *Astrobiology* 17:876–901.

Postberg, F., Kempf, S., Hillier, J.K., Srama, R., Green, S.F., McBride, N., and Grün, E. (2008) The E-ring in the vicinity of Enceladus: II. Probing the moon's interior—the composition of E-ring particles. *Icarus* 193:438–454.

Postberg, F., Kempf, S., Schmidt, J., Brilliantov, N., Beinsen, A., Abel, B., Buck, U., and Srama, R. (2009) Sodium salts in E-ring ice grains from an ocean below the surface of Enceladus. *Nature* 459:1098–1101.

Postberg, F., Schmidt, J., Hillier, J., Kempf, S., and Srama, R. (2011) A salt-water reservoir as the source of a compositionally stratified plume on Enceladus. Nature 474:620–622.Postberg, F., Khawaja, N., Abel, B., Choblet, G., Glein, C.R., Gudipati, M.S., Henderson, B.L., Hsu, H.-W., Kempf, S., Klenner, F., *et al.* (2018) Macromolecular organic compounds from the depths of Enceladus. *Nature* 558:564–568.

Rayman, M.D., Fraschetti, T.C., Raymond, C.A., and Russell, C.T. (2006) Dawn: a mission in development for exploration of main belt asteroids Vesta and Ceres. *Acta Astronaut* 58: 605–616.

Roth, L., Saur, J., Retherford, K.D., Strobel, D.F., Feldman, P.D., McGrath, M.A., and Nimmo, F. (2014) Transient water vapor at Europa's south pole. *Science* 343:171–174.

Rumble, J.R. (2018) Physical constants of organic compounds. In *CRC Handbook of Chemistry and Physics.*, edited by J.R. Rumble, CRC Press/Taylor & Francis, Boca Raton, FL.

Schaefer, R.T., MacAskill, J.A., Mojarradi, M., Chutjian, A., Darrach, M.R., Madzunkov, S.M., and Shortt, B.J. (2008) Digitally synthesized high purity, high-voltage radio frequency drive electronics for mass spectrometry. *Rev Sci Instrum* 79:095107.

Seidensticker, K.J., Möhlmann, D., Apathy, I., Schmidt, W., Thiel, K., Arnold, W., Fischer, H.-H., Kretschmer, M., Madlener, D., Péter, A., Trautner, R., and Schieke, S. (2007) SESAME—an experiment of the Rosetta lander Philae: objectives and general design. *Space Sci Rev* 128:301–337.

Sekine, Y., Shibuya, T., Postberg, F., Hsu, H.-W., Suzuki, K., Masaki, Y., Kuwatani, T., Mori, M., Hong, P.K., Yoshizaki, M., Tachibana, S., and Sirono, S.-i. (2015) High-temperature water–rock interactions and hydrothermal environments in the chondrite-like core of Enceladus. *Nat Commun* 6:8604.

Sephton, M.A. and Botta, O. (2005) Recognizing life in the solar system: guidance from meteoritic organic matter. *Int J Astrobiol* 4:269–276.

Sephton, M.A., Waite, J.H., and Brockwell, T.G. (2018) How to detect life on icy moons. *Astrobiology* 18:843–855.

Snyder, L.E., Lovas, F.J., Mehringer, D.M., Miao, N.Y., Kuan, Y.J., Hollis, J.M., and Jewell, P.R. (2002) Confirmation of interstellar acetone. *Astrophys J* 578:245–255.

Spahn, F., Schmidt, J., Albers, N., Hörning, M., Makuch, M., Seiß, M., Kempf, S., Srama, R., Dikarev, V., Helfert, S., Moragas-Klostermeyer, G., Krivov, A.V., Sremčević, M., Tuzzolino, A.J., Economou, T., and Grün, E. (2006) Cassini dust measurements at Enceladus and implications for the origin of the E ring. *Science* 311:1416–1418.

Sparks, W.B., Hand, K.P., McGrath, M.A., Bergeron, E., Cracraft, M., and Deustua, S.E. (2016) Probing for evidence of plumes on Europa with HST/STIS. *Astrophys J* 829:121.

Srama, R., Ahrens, T.J., Altobelli, N., Auer, S., Bradley, J.G., Burton, M., Dikarev, V.V., Economou, T., Fechtig, H., Görlich, M., Grande, M., Graps, A., Grün, E., Havnes, O., Helfert, S., Horanyi, M., Igenbergs, E., Jessberger, E.K., Johnson, T.V., Kempf, S., Krivov, A.V., Krüger, H., Mocker-Ahlreep, A., Moragas-Klostermeyer, G., Lamy, P., Landgraf, M., Linkert, D., Linkert, G., Lura, F., McDonnell, J.A.M., Möhlmann, D., Morfill, G.E., Müller, M., Roy, M., Schäfer, G., Schlotzhauer, G., Schwehm, G.H., Spahn, F., Stübig, M., Svestka, J., Tschernjawski, V., Tuzzolino, A.J., Wäsch, R., and Zook, H.A. (2004) The Cassini cosmic dust analyzer. *Space Sci Rev* 114:465–518.

Stein, S.E. (2018) Mass spectra: NIST MS #228221. In *NIST Chemistry Webbook, NIST Standard Reference Database*, edited by P.J. Linstrom and W.G. Mallards, National Institute of Standards and Technology, Gaithersberg, MD.

Tomasko, M.G., Archinal, B., Becker, T., Bézard, B., Bushroe, M., Combes, M., Cook, D., Coustenis, A., de Bergh, C., Dafoe, L.E., Doose, L., Douté, S., Eibl, A., Engel, S., Gliem, F., Grieger, B., Holso, K., Howington-Kraus, E., Karkoschka, E., Keller, H.U., Kirk, R., Kramm, R., Küppers, M., Lanagan, P., Lellouch, E., Lemmon, M., Lunine, J., McFarlane, E., Moores, J., Prout, G.M., Rizk, B., Rosiek, M., Rueffer, P., Schröder, S.E., Schmitt, B., See, C., Smith, P., Soderblom, L., Thomas, N., and West, R. (2005) Rain, winds and haze during the Huygens probe's descent to Titan's surface. *Nature* 438:765–778.

Waite, J.H., Lewis, W.S., Kasprzak, W.T., Anicich, V.G., Block, B.P., Cravens, T.E., Fletcher, G.G., Ip, W.-H., Luhmann, J.G., McNutt, R.L., Niemann, H.B., Parejko, J.K., Richards, J.E., Thorpe, R.L., Walter, E.M., and Yelle, R.V. (2004) The cassini ion and neutral mass spectrometer (INMS) investigation. *Space Sci Rev* 114:113–231.

Waite, J.H., Niemann, H., Yelle, R.V., Kasprzak, W.T., Cravens, T.E., Luhmann, J.G., McNutt, R.L., Ip, W.-H., Gell, D., De La Haye, V, Müller-Wordag, I., Magee, B., Borggren, N., Ledvina, S., Fletcher, G., Walter, E., Miller, R., Scherer, S., Thorpe, R., Xu, J., Block, B., and Arnett, K. (2005) Ion neutral mass spectrometer results from the first flyby of Titan. *Science* 308:982–986.

Waite, J.H., Combi, M.R., Ip, W.-H., Cravens, T.E., McNutt, R.L., Kasprzak, W., Yelle, R., Luhmann, J., Niemann, H., Gell, D., Magee, B., Fletcher, G., Lunine, J., and Tseng, W.-L. (2006) Cassini ion and neutral mass spectrometer: enceladus plume composition and structure. *Science* 311:1419–1422.

Waite, J.H., Lewis, W.S., Magee, B.A., Lunine, J.I., McKinnon, W.B., Glein, C.R., Mousis, O., Young, D.T., Brockwell, T., Westlake, J, Nguyen, M.J., Teolis, B.D., Niemann, H.B., McNutt Jr, R.L., Perry, M., and Ip, W.H. (2009) Liquid water on Enceladus from observations of ammonia and ^{40}Ar in the plume. *Nature* 460:487–490.

Waite, J.H., Glein, C.R., Perryman, R.S., Teolis, B.D., Magee, B.A., Miller, G., Grimes, J., Perry, M.E., Miller, K.E., Bouquet, A, Lunine, J.I., Brockwell, T., and Bolton, S.J. (2017) Cassini finds molecular hydrogen in the Enceladus plume: evidence for hydrothermal processes. *Science* 356:155–159.

Webster, C.R., Mahaffy, P.R., Atreya, S.K., Moores, J.E., Flesch, G.J., Malespin, C., McKay, C.P., Martinez, G., Smith, C.L., Martin-Torres, J. Gomez-Elvira, J., Zorzano, M.-P., Wong, M.H., Trainer, M.G., Steele, A., Archer, D., Sutter, B., Coll, P.J., Freissinet, C., Meslin, P.-Y., Gough, R.V., House, C.H., Pavlov, A., Eigenbrode, J.L., Glavin, D.P., Pearson, J.C., Keymeulen, D., Christensen, L.E., Schwenzer, S.P., Navarro-Gonzalez, R., Pla-García, J., Rafkin, S.C.R., Vicente-Retortillo, Á., Kahanpää, H., Viudez-Moreiras, D., Smith, M.D., Harri, A.-M., Genzer, M., Hassler, D.M., Lemmon, M., Crisp, J., Sander, S.P., Zurek, R.W., and Vasavada, A.R. (2018) Background levels of methane in Mars' atmosphere show strong seasonal variations. *Science* 360:1093–1096.

Address correspondence to:
Joshua S. Wiley
Electrophoretic Mass Spectrometry
Technology (EMAST) Corp.
11990 Heritage Oak Pl
Suite 3
Auburn, CA 95603

E-mail: joshua.wiley@cmpscientific.com

Abbreviations Used

AA = amino acid
Ala = alanine
CDA = cosmic dust analyzer
CI = chemical ionization
CI-MS = chemical ionization mass spectrometry
EI = electron impact ionization
EI-MS = electron impact ionization mass spectrometry
FA = fatty acid
Gly = glycine
ID = inner diameter
II = impact ionization
INMS = ion and neutral mass spectrometer
JPL = Jet Propulsion Lab
LA = lauric acid
LAH$^+$ = protonated lauric acid
m/z = mass-to-charge
MASPEX = Mass Spectrometer for Planetary Exploration
Met = methionine
MOMA = Mars Organic Molecule Analyzer
MS/MS = Mass Spectrometry/Mass Spectrometry
(aka tandem MS)
NIST = National Institute for Standards
and Technology
OD = outer diameter
PA = proton affinity
Phe = phenylalanine
QITMS = Quadrupole Ion Trap Mass Spectrometer
RF = radio frequency
S.A.M = Spacecraft Atmosphere Monitor
SAM QMS = Surface Analysis at Mars Quadrupole
Mass Spectrometer
Ser = serine
*Ser*H$^+$ = protonated serine
SUDA = Surface Dust Analyzer
VCAM = Vehicle Cabin Atmosphere Monitor